(35) Burell, H. In *Polymer Handbook*, 2nd ed.; Brandrup, J.; Immergut, E. H.; Eds.; Wiley: New York, 1975; p IV-341.

(36) Gauthier, S.; Duchesne, D.; Eisenberg, A. *Macromolecules* **1987**, *20*, 753.

Thermodynamic Predictions of Volume Changes in Temperature-Sensitive Gels. 1. Theory

M. Marchetti, S. Prager,[†] and E. L. Cussler[*]

Department of Chemical Engineering and Materials Science, University of Minnesota, Minneapolis, Minnesota 55455. *Received May 30, 1989;*
Revised Manuscript Received October 10, 1989

ABSTRACT: This paper presents a molecular theory of swollen gels based on a compressible lattice model. The theory extends the Sanchez and Lacombe lattice-fluid model for polymer solutions through addition of the elastic term of the Flory–Rehner theory of rubber swelling. The characterization of this type of binary mixture requires knowledge of pure component parameters and an interaction energy correction characteristic of each binary mixture. The four basic types of liquid–gel phase diagrams predicted are related to the presence of upper and lower consolute temperatures or closed immiscibility loops in solution of the uncross-linked polymer.

Introduction

Temperature-sensitive gels can be used to concentrate dilute solutions or to alter drug release. For example, such gels have been used to produce soy protein isolate[1,2] and to alter insulin release.[3-5] As such, they are a new technology of practical significance.

These gels swell when they are placed in water. The swelling occurs because the polymer is hydrophilic; it is constrained because of chemical cross-links present between the polymer chains. However, the swelling varies sharply with temperature. For example, poly(isopropylacrylamide) gel swells to 30 times its dry volume in water at 34 °C but only 4 times its dry volume at 35 °C.[1,6]

Such violent changes in swelling occur because of the proximity of a consolute point in the homologous uncross-linked polymer. They can be induced by changes in pH,[7] by the application of electrical fields,[8] by the addition of mixed solvents,[9] or by pressure.[10]

A theory of these swelling transitions must include both the solution characteristics of the uncross-linked polymer chains and the elastic effects introduced by the cross-links. The experimental phase diagram of Figure 1 illustrates both features. The uncross-linked polymer is shown as squares, and the cross-linked gel is shown as triangles. The region above the squares is a two-phase region, consisting of a water-rich phase and a polymer-rich phase. Below 31 °C, the polymer and water are completely miscible; above this temperature they become only partially miscible. The minimum on this curve is a "lower consolute point" or "lower critical solution temperature" (LCST).

The phase behavior of the gel above 34 °C is like that of the uncross-linked polymer, forming pure water and a polymer-rich phase. The pure water phase contains no gel because the presence of cross-links does not allow the complete dissolution of the gel. The gel below 34 °C may exist as a homogeneous gel phase or as a highly swollen gel in equilibrium with excess water.[2,11]

The behavior in Figure 1 is part of the general behavior of uncross-linked polymers shown in Figure 2.[12-14] Of the three two-phase regions A, B, and C shown there, only the lower portion of C, including the critical point labeled LCSTII, is covered by the temperature range of Figure 1. Region A is the normal-phase separation predicted by the original Flory–Huggins model. Here polymer–solvent miscibility is governed by the energy of forming contacts between polymer segments and solvent at essentially constant volume, even under constant pressure conditions. The dominant consideration in region B is that the solvent is approaching the critical point of its liquid–vapor curve; mixing at constant pressure here produces large changes in the total volume. In region C, miscibility is determined by a complex interplay between polymer–solvent interactions and volume changes. Part of the complexity arises from the fact that the thermodynamic functions both of the mixture and of the pure components are affected in nontrivial ways by thermal expansion.

These considerations have been developed along rather different lines into quantitative theories by Flory[14] and by Sanchez and Lacombe.[15] In this paper we combine the more tractable model of Sanchez and Lacombe with Flory's treatment of network swelling to obtain a theory of swelling transitions. Comparison with experiment will be the subject of a second paper.

Theory

The starting points for the model of this gel are the Sanchez and Lacombe theory of mixing and the Flory–Rehner theory of rubber elasticity.[14-16] The gel's partition function is as a first approximation separated into elastic and mixing factors,[17-19] and the Helmholtz free

---

[†] Department of Chemistry, University of Minnesota, Minneapolis, MN 55455.

0024-9297/90/2223-1760$02.50/0

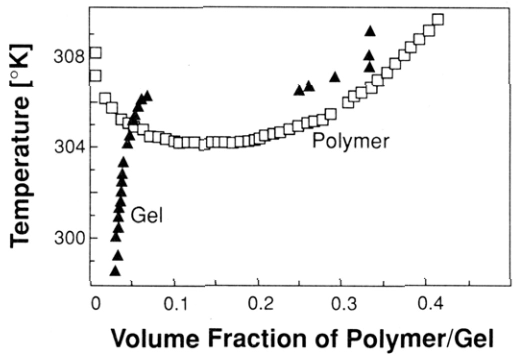

Figure 1. Isobaric phase diagram for poly(isopropylacrylamide) polymer and gel.

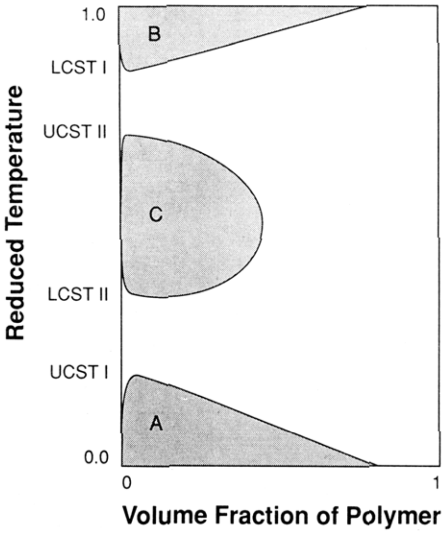

Figure 2. Schematic representation of probable phase behavior of uncross-linked polymers.

energy for the swollen gel is the sum of a mixing and an elastic term:

$$\Delta F = \Delta F_M + \Delta F_E \tag{1}$$

The Helmholtz free energy of mixing ΔF_M is given by the Sanchez and Lacombe extension to the Flory–Huggins theory of polymer–solvent systems.[15,20,21] The original lattice models like that of Flory and Rehner require that every site is occupied by a molecule or a segment of a molecule, so that the volume of the system is completely specified by the amounts of each species present. Such incompressible lattice theories cannot predict lower consolute points, since these phenomena generally involve nonzero volumes of mixing.[20–25] Volume changes are built into the theory by including lattice vacancies or holes as a third component (the zeroth component): The introduction of holes, which is not our invention, is one way to allow for nonzero volumes of mixing while conserving the simplicity of the lattice representation.

The elastic free energy ΔF_E due to the cross-links is responsible for the rubberlike behavior of gels, which are capable of undergoing large strains without suffering permanent deformation.[14,26] The elastic behavior is described by the ideal phantom network model for non-ionic systems.[17,26,27]

Free Energy of Mixing. The original Flory–Huggins theory predicts only an upper critical solution temperature for endothermic mixtures. To remedy this, past workers, including Flory himself,[24] have relaxed the incompressibility constraint used in the formation of the mixing phenomena.

Flory's original formulation of the free energy of mixing for a binary incompressible mixture is[14]

$$\frac{\Delta F_M}{kT} = n_s \ln \phi_s + n_g \ln \phi_g + v_s^* n_s \chi_{sg}' \phi_g \tag{2}$$

where n_s and n_g are the number of molecules of solvent and polymer, respectively, ϕ_s and ϕ_g are their respective site fractions, and v_s^* is the close-packed volume of a solvent molecule (i.e., the molecular volume of the solvent well below its boiling point). The interaction parameter per lattice site χ_{sg}' is defined as

$$\chi_{sg}' = \frac{1}{kT}[((P_s^*)^{1/2} - (P_g^*)^{1/2})^2 + 2Z_{sg}(P_s^* P_g^*)^{1/2}] \tag{3}$$

where P_s^* and P_g^* are the cohesive energy densities for the solvent and gel, respectively, and Z_{sg} is a correction parameter characterizing the mixture.

The lattice can be made compressible by introducing a third component: the vacant sites or holes. Holes act as a nonsolvent for the gel, with zero cohesive energy density (i.e. $P_0^* = 0$); the new interaction energy parameters χ_{s0}' and χ_{g0}' are given by

$$\chi_{s0}' = P_s^*/kT \tag{4}$$

$$\chi_{g0}' = P_g^*/kT \tag{5}$$

and the mixing free energy becomes

$$\frac{\Delta F_M}{kT} = n_s \ln \phi_s + n_g \ln \phi_g + v_s^* n_s \chi_{sg}' \phi_g + n_0 \ln \phi_0 + v_0^*[n_0 \chi_{s0}' \phi_s + n_0 \chi_{g0}' \phi_g] \tag{6}$$

where n_0 and ϕ_0 are the number and fraction of empty sites, respectively, and v_0^* is the empty lattice site volume.

The close-packed volumes and cohesive energy densities are physical parameters that can be obtained from pure component data. The volume of an empty lattice site is determined by choosing v_0^* so as to fit the observed P–V–T data for the pure solvent. (In this respect, our treatment differs from that of Sanchez and Lacombe, who allow v_0^* to vary with the composition of the mixture.[15,20–22]) There is only one adjustable parameter characterizing the mixture: the deviation Z_{sg} from the Hildebrand mixing rule.

Elastic Free Energy. The deformation which occurs during swelling is considered to take place without appreciable changes in the internal energy of the gel structure. Thus, the free energy change ΔF_E is purely entropic: the entropy change corresponds to the decrease of the number of configurations allowed to the network chains as the gel volume increases.[14,17] Since the gel is synthesized in solution, the elastic free energy for a tetrafunctional network is

$$\frac{\Delta F_E}{kT} = \frac{3}{2}\nu\left[\left(\frac{\phi_g}{\phi_g^0}\right)^{-2/3} - 1\right] \tag{7}$$

where ν is the number of cross-links in the network and ϕ_g^0 is the volume fraction of gel under synthesis conditions. The ratio ϕ_g/ϕ_g^0 must represent the swelling of the network relative to its *unstressed* state, i.e., the state at the time the cross-links were introduced. In the standard theory it is tacitly assumed that synthesis takes place in the absence of diluent, in which case theta conditions would apply. The polyacrylamide gels under discussion however, are synthesized in aqueous solution and are therefore already partially swollen in their unstressed state. In addition, eq 7 does not contain the logarithmic expression found in Flory's development: the cross-links are not free to explore the volume of the system.[14] The only physical parameter involved in the elastic contribution is the number of cross-links per unit volume of gel, a quantity which is experimentally accessible.[14,28]

Free Energy of Swollen Networks. We now combine eqs 6 and 7 to find the Helmholtz free energy per unit volume for swelling a gel

$$\frac{\Delta F}{kTV} = \phi_{\mathrm{s}}\left[\frac{1}{v_{\mathrm{s}}^*}\ln\phi_{\mathrm{s}} + \chi_{\mathrm{sg}}'\phi_{\mathrm{g}}\right] + \frac{3}{2}\frac{\nu}{V_{\mathrm{g}}^*}[\phi_{\mathrm{g}}^{1/3}(\phi_{\mathrm{g}}^0)^{2/3} - \phi_{\mathrm{g}}] + \phi_0\left[\frac{1}{v_0^*}\ln\phi_0 + \chi_{\mathrm{s0}}'\phi_{\mathrm{s}} + \chi_{\mathrm{g0}}'\phi_{\mathrm{g}}\right] \quad (8)$$

where (ν/V_{g}^*) is the number of cross-links per unit volume of dry unswollen gel. The total volume of the system V is

$$V = n_0v_0^* + n_{\mathrm{s}}v_{\mathrm{s}}^* + V_{\mathrm{g}}^* \quad (9)$$

The experimental close-packed volume fractions of solvent and polymer are readily converted to compressible lattice site fractions

$$\phi_i = (1 - \phi_0)v_i \quad (10)$$

where v_i is the normal close-packed volume fraction of i given by

$$v_i = n_iv_i^*/\sum_{j=1}^{2} n_jv_j^* \quad (11)$$

The close-packed volume v_i^* is related to the hard core mass density ρ_i^* and molecular weight of component i, M_i, by

$$v_i^* = M_i/\rho_i^* \quad (12)$$

so that

$$v_i = (n_iM_i/\rho_i^*)/\sum(n_jM_j/\rho_j^*) \quad (13)$$

If the hard-core densities of the components (ρ_i^*) are not too different, we may replace the volume fractions in eq 13 by weight fractions. While the composition units used above may not seem the familiar mole or volume fractions, the nature of the lattice model makes it more convenient to use the fractions ϕ_i of total sites, including vacancies, as the composition variables. In the case of polymer networks the experimentally used variable is the swelling ratio q equal to the ratio of the volumes of the swollen and unswollen structures,[14] $V/V_{\mathrm{g}}^* = 1/\phi_{\mathrm{g}}$.

Expressions for the chemical potentials can be derived in a straightforward manner from eq 8. The chemical potentials for the solvent and for the gel are given by

$$\frac{\mu_{\mathrm{s}}}{v_{\mathrm{s}}^*kT} = \frac{1}{v_{\mathrm{s}}^*}\left[\ln\phi_{\mathrm{s}} + \left(1 - \frac{v_{\mathrm{s}}^*}{v_0^*}\right)\phi_0 + \phi_{\mathrm{g}}\right] + \frac{\nu\phi_{\mathrm{g}}^0}{V_{\mathrm{g}}^*}\left(\frac{\phi_{\mathrm{g}}}{\phi_{\mathrm{g}}^0}\right)^{1/3} + [\chi_{\mathrm{sg}}'\phi_{\mathrm{g}} + \chi_{\mathrm{s0}}'\phi_0](\phi_0 + \phi_{\mathrm{g}}) - \chi_{\mathrm{g0}}'\phi_0\phi_{\mathrm{g}} \quad (14)$$

$$\frac{\mu_{\mathrm{g}}}{v_{\mathrm{g}}^*kT} = -\frac{\phi_{\mathrm{s}}}{v_{\mathrm{s}}^*} - \frac{\phi_0}{v_0^*} + \frac{\nu\phi_{\mathrm{g}}^0}{V_{\mathrm{g}}^*}\left(\frac{\phi_{\mathrm{g}}}{\phi_{\mathrm{g}}^0}\right)^{1/3} + (\chi_{\mathrm{sg}}'\phi_{\mathrm{s}} + \chi_{\mathrm{g0}}'\phi_0)(\phi_{\mathrm{s}} + \phi_0) - \chi_{\mathrm{s0}}'\phi_{\mathrm{s}}\phi_0 \quad (15)$$

An equation of state for the system is obtained in the form of the chemical potential for the holes (μ_0), essentially the pressure acting on the system

$$P = -\frac{1}{v_0^*}\left[\frac{\partial\Delta F}{\partial n_0}\right]_{n_{\mathrm{s}},n_{\mathrm{g}},V,T} = -\frac{\mu_0}{v_0^*} \quad (16)$$

so that

$$P = -kT\left\{\frac{1}{v_0^*}\left[\ln\phi_0 + \left(1 - \frac{v_0^*}{v_{\mathrm{s}}^*}\right)\phi_{\mathrm{s}} + \phi_{\mathrm{g}}\right] + \frac{\nu\phi_{\mathrm{g}}^0}{V_{\mathrm{g}}^*}\left(\frac{\phi_{\mathrm{g}}}{\phi_{\mathrm{g}}^0}\right)^{1/3} + [\chi_{\mathrm{s0}}'\phi_{\mathrm{s}} + \chi_{\mathrm{g0}}'\phi_{\mathrm{g}}](\phi_{\mathrm{s}} + \phi_{\mathrm{g}}) - \chi_{\mathrm{sg}}'\phi_{\mathrm{s}}\phi_{\mathrm{g}}\right\} \quad (17)$$

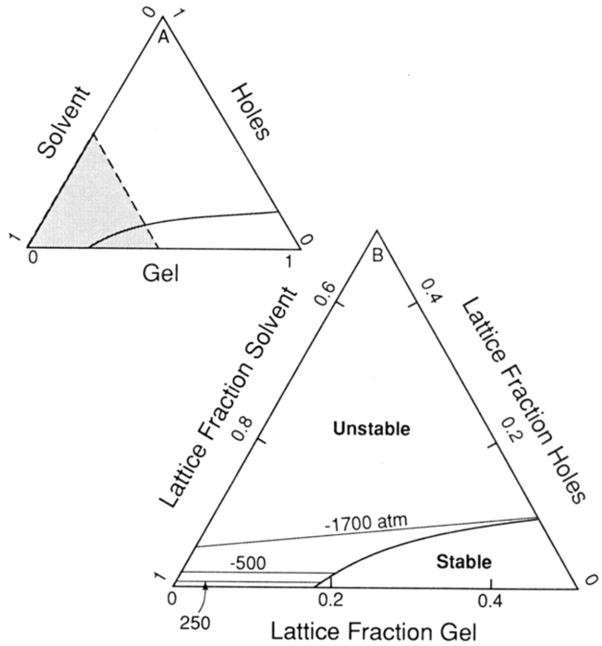

Figure 3. Isothermal spinodals for a compressible swollen gel ($P_{\mathrm{s}}^*/P_{\mathrm{g}}^* = 1.25$, $v_0^* = 17.12$, $Z_{\mathrm{sg}} = 0.0105$, $\nu/v_{\mathrm{g}}^* = 10^{-6}$). *B* corresponds to the shaded region of A.

A system containing a cross-linked gel differs from a true solution in that only solvent molecules (and holes) can redistribute themselves between phases. The network performs the dual role of a solute and an osmotic membrane, since it is not free to enter the solvent-rich phase.[14] Thus the total number of gel molecules in the gel phase remains constant.

The equations given above allow calculation of both spinodal and binodal curves. The spinodal condition for this kind of physical picture is

$$\left[\frac{\partial^2\Delta F}{\partial\phi_{\mathrm{s}}^2}\right]_{T,V,\varphi_0}\left[\frac{\partial^2\Delta F}{\partial\phi_0^2}\right]_{T,V,\varphi_{\mathrm{s}}} - \left[\frac{\partial}{\partial\phi_{\mathrm{s}}}\left(\frac{\partial\Delta F}{\partial\phi_0}\right)_{T,V,\varphi_{\mathrm{s}}}\right]_{T,V,\varphi_0}^2 = 0 \quad (18)$$

In explicit terms, eq 18 becomes

$$\left[\frac{1}{v_{\mathrm{s}}^*\phi_{\mathrm{s}}} - 2\chi_{\mathrm{sg}}'\right]\left[\frac{1}{v_0^*\phi_0} - 2\chi_{\mathrm{g0}}'\right] - [\chi_{\mathrm{s0}}' - \chi_{\mathrm{g0}}' - \chi_{\mathrm{sg}}']^2 = 0 \quad (19)$$

Equation 19 gives the local stability limits for the gel at a fixed temperature and volume. Note that no elastic terms are present in the spinodal decomposition.

Typical spinodals found from eq 19 by the Newton–Raphson method are shown in Figure 3, corresponding to a region of partial miscibility near an upper critical solution boundary. Note that the pressure is not constant in this figure; it varies along the spinodals where equal pressure tie lines have been indicated. Most of the figure corresponds to negative pressures at which the system would be under tension; only for empty lattice fractions below 1% does one encounter positive pressures along the spinodals. To find the spinodal envelope at constant pressure, two changes are necessary: we must obtain curves representing isobaric stability limits by "stacking" isothermal diagrams and then convert the associated lattice fractions of Figure 3 to the physically measured volumetric fractions by means of eq 10.

The equilibrium binodal for the system is calculated at a fixed temperature by equating the pressure and the solvent chemical potentials in the coexisting phases. By assuming the solvent to be in excess, we find a compressible swollen gel phase in equilibrium with a compressible solvent phase. To obtain the isobaric binodals, we first choose a pressure and then solve eq 17 for the density of the gel-free phase coexisting with the swollen gel. We need then solve only the remaining solvent-gel equilibrium conditions

$$\mu_0{}^{\mathrm{G}}(\phi_0{}^{\mathrm{G}},\phi_{\mathrm{s}}{}^{\mathrm{G}};T) - \mu_0{}^{\mathrm{S}}(\phi_{\mathrm{s}}{}^{\mathrm{S}},T) = 0 \tag{20}$$

$$\mu_{\mathrm{s}}{}^{\mathrm{G}}(\phi_0{}^{\mathrm{G}},\phi_{\mathrm{s}}{}^{\mathrm{G}};T) - \mu_{\mathrm{s}}{}^{\mathrm{S}}(\phi_{\mathrm{s}}{}^{\mathrm{S}},T) = 0 \tag{21}$$

The superscripts G and S refer to the swollen gel and the gel-free phases, respectively; the chemical potentials are defined by eq 14 and 17. Again, the solution of these nonlinear equations is carried out by the Newton–Raphson method. Generation of the isobar is performed by using first-order continuation in temperature. Details of these calculations are given elsewhere.[29]

Each binodal calculation at a given temperature and pressure corresponds to a single tie line in Figure 3. The final results for the isobar are again changed to the physically measured fractions by use of eq 10. Multiple solutions are resolved by global free energy minimization.

Results

In general, the predicted phase diagram is a function of six parameters: the cohesive energy densities for the solvent $P_{\mathrm{s}}{}^*$ and for the gel $P_{\mathrm{g}}{}^*$, the correction parameter Z_{sg} characterizing the mixture, the close-packed volume of the solvent $\upsilon_{\mathrm{s}}{}^*$, the volume of the vacant site $\upsilon_0{}^*$, and the density of cross-links at synthesis $\nu(\phi_{\mathrm{g}}{}^0)^{2/3}/V_{\mathrm{g}}{}^*$. Three parameters, $\upsilon_{\mathrm{s}}{}^*$, $\upsilon_0{}^*$, and $P_{\mathrm{s}}{}^*$, are found from the vapor-liquid P–V–T equilibrium binodal of the pure solvent as described by Sanchez and Lacombe.[20] The value of $P_{\mathrm{g}}{}^*$ may be found from the heat of phase transition by use of differential scanning calorimetry as indicated in a second paper. The value of $\nu(\phi_{\mathrm{g}}{}^0)^{2/3}/V_{\mathrm{g}}{}^*$ may be found experimentally by measuring the elastic modulus of the gel. The remaining parameter Z_{sg} is adjusted to fit the phase envelope of the swollen gel at the volume transition region.

The general features of the liquid–gel phase diagram can be summarized in the following manner. Comparing our formulation of the chemical potential of the solvent as given by eq 14 to the classical Flory–Rehner theory

$$\frac{\mu_{\mathrm{s}}}{\upsilon_{\mathrm{s}}{}^*kT} = \frac{1}{\upsilon_{\mathrm{s}}{}^*}[\ln \upsilon_{\mathrm{s}} + \upsilon_{\mathrm{g}} + \chi_{\mathrm{s}}\upsilon_{\mathrm{g}}{}^2] + \frac{\nu\upsilon_{\mathrm{g}}{}^0}{V_{\mathrm{g}}{}^*}\left(\frac{\upsilon_{\mathrm{g}}}{\upsilon_{\mathrm{g}}{}^0}\right)^{1/3} \tag{22}$$

Assuming that $\upsilon_{\mathrm{g}}{}^0 = \phi_{\mathrm{g}}{}^0$, the subtraction of eq 22 from eq 14 yields an expression for the interaction parameter χ_{s} in terms of the treatment presented above. This parameter, defined on a solvent molecule basis, is now a function of the free volume of the mixture and includes both entropic and energetic contributions

$$\chi_{\mathrm{s}} = \left[\frac{1-\phi_0}{\phi_{\mathrm{g}}}\right]^2 \left\{ \ln(1-\phi_0) + \phi_0\left(1 - \frac{\upsilon_{\mathrm{s}}{}^*}{\upsilon_0{}^*} - \frac{\phi_{\mathrm{g}}}{1-\phi_0}\right) + \upsilon_{\mathrm{s}}{}^*\left[-\frac{\nu\phi_{\mathrm{g}}{}^0}{V_{\mathrm{g}}{}^*}\left(\frac{\phi_0\phi_{\mathrm{g}}}{\phi_{\mathrm{g}}{}^0(1-\phi_0)}\right)^{1/3} + (\chi_{\mathrm{sg}}{}'\phi_{\mathrm{g}} + \chi_{\mathrm{s0}}{}'\phi_0)(\phi_{\mathrm{g}} + \phi_0) - \chi_{\mathrm{g0}}\phi_{\mathrm{g}}\phi_0\right]\right\} \tag{23}$$

The variation of χ_{s} is clearly a complex function of both volume fractions and gel elasticity.

Equation 23 leads to four different types of phase diagrams shown in the four parts of Figure 4. Each part of this figure gives the variation of χ_{s} with reduced temperature, the phase diagram of the uncross-linked polymer, and the phase diagram of the gel. As a result, each part is a theoretical generalization to the results in Figures 1 and 2.

The four different parts of Figure 4 refer to four different ranges of parameters

(A) $P_{\mathrm{s}}{}^*/P_{\mathrm{g}}{}^* \cong 1$, $\Theta_{\mathrm{u}} \geq 0$
(B) $P_{\mathrm{s}}{}^*/P_{\mathrm{g}}{}^* > 1$, $\Theta_{\mathrm{u}} \geq 0$
(C) $P_{\mathrm{s}}{}^*/P_{\mathrm{g}}{}^* \cong 1$, $\Theta_{\mathrm{u}} < 0$
(D) $P_{\mathrm{s}}{}^*/P_{\mathrm{g}}{}^* > 1$, $\Theta_{\mathrm{u}} > 0$

where Θ_{u} is the temperature at which $\chi_{\mathrm{sg}}{}' = 1/2$ for the corresponding solvent–uncross-linked polymer pair. In all parts of Figure 4, the lower consolute boundary corresponding to region B in Figure 2 is predicted. However, its appearance may be obscured if the cross-linking degree is too high or if the intermediate miscibility region C of Figure 2 is too large. Although all four types of phase diagrams are possible, only portions of these diagrams are commonly observed. Boiling or freezing of the mixture also limits the observation range, and freezing is not included in the present theory.

Cases A and B reflect different choices of cohesive energy density ratios. Figure 5 shows a more direct comparison of these two cases. When $P_{\mathrm{s}}{}^*/P_{\mathrm{g}}{}^* = 1$ the solvent and gel have similar cohesive energy densities, and the predicted phase behavior corresponds to that normally encountered with non-polar uncross-linked polymers. The resulting phase diagram shows an upper consolute region at low reduced temperature ($T_{\mathrm{r}} < 0.32$) and a lower consolute one near the critical temperature of the solvent ($T_{\mathrm{r}} > 0.95$) associated with the consolute boundaries A and B presented in Figure 2. These regions are also indicated as A and B in Figure 5. The intermediate behavior, which shows no miscibility gap like that in Figure 2, is a result of the elastic effects caused by the presence of cross-links.

The appearance and location of the upper consolute region is mainly influenced by the value of Z_{sg}. This choice, which determines the value of Θ_{u} (above or below 0 K), is the feature that differentiates cases A and C from cases B and D in Figure 4. An actual upper consolute point is not seen in the case of cross-linked gels, since the system cannot reach the infinite dilution limit. The second consolute gap, due to free volume dissimilarities between solvent and gel, also does not show the associated lower consolute point due to the presence of cross-links.

When the solvent has a much larger cohesive energy density than the gel, the solution phase behavior is quite different. This case is exemplified by the curve for $P_{\mathrm{s}}{}^*/P_{\mathrm{g}}{}^* = 2$, also shown in Figure 5 (case B in Figure 4). As

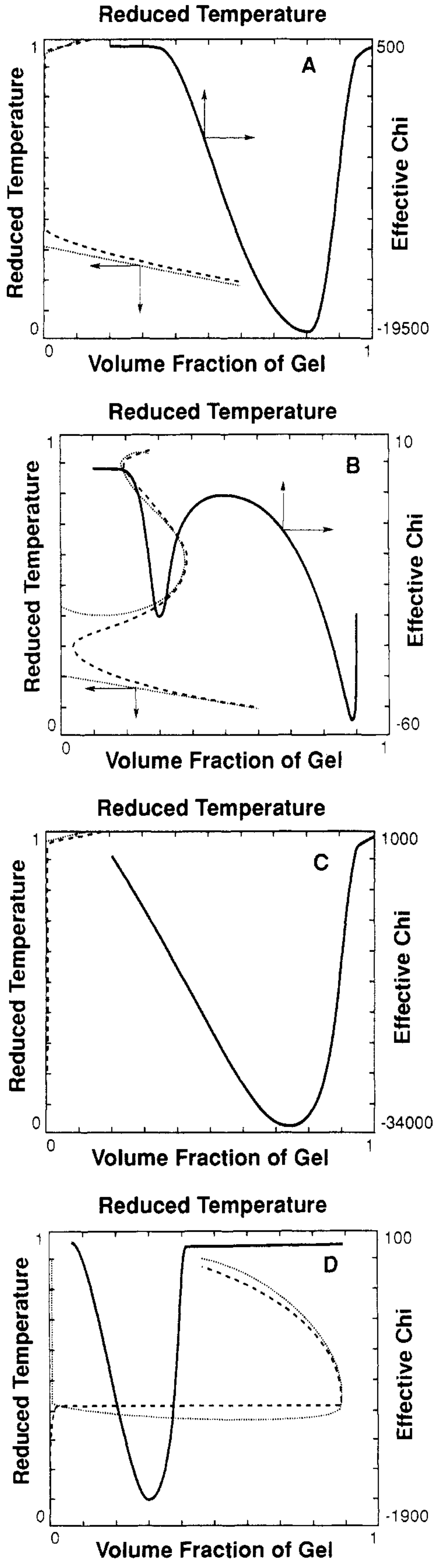

Figure 4. Calculated liquid–gel phase diagrams. The dashed lines for the gel phase diagrams are complemented by the dotted lines for the uncross-linked polymer phase diagrams. The solid lines give the value of χ_s.

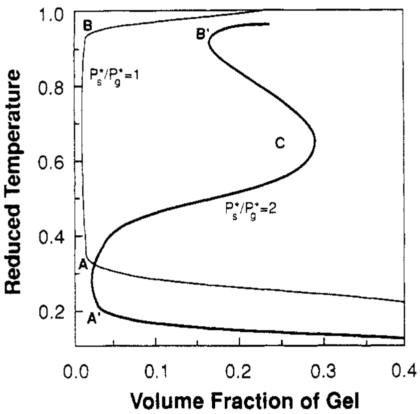

Figure 5. Effect of cohesive energy density ratios on the predicted equilibrium phase behavior (reduced temperature = T/T_c^s).

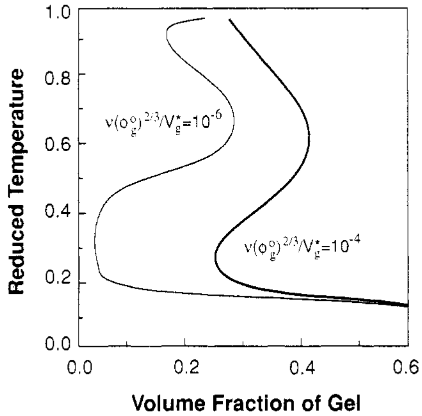

Figure 6. Effect of cross-link density on the predicted equilibrium phase behavior (reduced temperature = T/T_c^s).

before, there is an upper consolute boundary, at a reduced temperature below 0.2 (indicated as A′), and a lower consolute boundary, now above a reduced temperature of 0.92 (indicated as B′). There is in addition a central region dominated by mixing effects (indicated as C), with a second upper consolute transition near $T_r = 0.85$ and a second lower consolute transition near $T_r = 0.42$. These effects correspond to the closed loop miscibility gap presented in Figure 2. The lower part of this region (indicated as C in Figures 2 and 5) is the basis of the gel separation process, which occurs at moderate temperatures, away from the critical region of the solvent. This second region is observed only in polar systems, and it is due to site-specific interactions such as hydrogen bonds.[12] Increasing the cohesive energy density ratio (P_s^*/P_g^*) expands region C until it becomes the principal feature of the resulting phase behavior.

Cases C and D in Figure 4 compare the effect of different cohesive energy density ratios ($P_s^*/P_g^* = 1$ and 2.5) for situations where $\Theta_u < 0$ K. In these two cases, the consolute boundary corresponding to region A of Figure 2 has disappeared from the predicted phase diagrams shown in Figure 4 due to the choice of Z_{sg}. This parameter affects most directly the location of Θ_u.

The cross-link density strongly influences the gel volume fraction at which the elastic effects dominate the phase behavior of the system. As shown in Figure 6, high cross-linking causes the elastic contribution to appear at larger volume fractions of gel. The two binodals shown there, constructed for a cohesive energy density ratio of 2, have cross-linking densities of 10^{-6} and 10^{-4} mol/cm^3 of gel at synthesis conditions. In the less densely cross-linked gel we can attain a swelling some 10 times larger than in the more densely cross-linked network. With increasing number of cross-links, the consolute region corresponding to B in Figure 2 becomes obscured, and the intermediate region (C in Figures 2 and 4) shows a smaller volume change than that expected for the weakly cross-linked gel.

Pressure also has a dramatic effect on the shape of these diagrams. Both the intermediate miscibility gap and the high-temperature lower consolute boundary can be completely erased if the pressure is increased sufficiently, consistent with the behavior observed in uncross-linked polymers.[15,20-25] In contrast, the low-temperature upper consolute boundary is generally insensitive to variations in the pressure of the system.

Conclusions

This paper develops a molecular theory to explain the solution behavior of hydrogels. This development explicitly includes free volume as a third component in the binary mixture, so that an equation of state for the system can be derived. The phase behavior predicted for swollen gels includes near-critical lower consolute boundaries, low-temperature upper consolute boundaries, and closed-loop miscibility gaps potentially containing additional lower and upper consolute boundaries. The theory has one adjustable parameter: the interaction energy correction Z_{sg}. Other parameters are either experimentally accessible or can be determined from pure component properties. These results are consistent with those obtained for uncross-linked polymers using theories such as the Flory and Orwoll cell model, the Koningsveld and Kleintjens hole theory, and the Sanchez and Lacombe lattice fluid theory.[15,20-22,24]

However, while this theory shows interesting qualitative behavior, it has not been compared with experiment. In particular, the parameters involved in using the theory have not been quantitatively evaluated. In addition, the approach taken here merits comparison with other theoretical efforts aimed at the same phenomena.[30-32] We make both comparisons for cross-linked poly(isopropylacrylamide) and other related hydrogels in a subsequent paper.

Acknowledgment. This work was partially supported by the National Science Foundation (Grant NF/CBT 86-11646) and by the Hoechst Celanese Corp.

References and Notes

(1) Freitas, R. F. S.; Cussler, E. L. *Sep. Sci. Technol.* **1987**, *22*, 911.

(2) Trank, S. J.; Johnson, D. W.; Cussler, E. L. *J. Food Technol.* **1989**, *24* (6), 780.

(3) Hoffman, A. S.; Afrassiabi, A.; Dong, L. C. *J. Controlled Release* **1986**, *4*, 213.

(4) Dong, L. C.; Hoffmann, A. S. *J. Controlled Release* **1986**, *4*, 223.

(5) Siegel, R. A.; Firestone, B.; Falamarzian, M. AIChE Washington Meeting (Nov), 1988, paper 122h.

(6) Ilavsky, M.; Hrouz, J.; Ulbrich, K. *Polym. Bull.* **1982**, *7*, 107.

(7) Cussler, E. L.; Stokar, M. R.; Vaarberg, J. E. *AIChE J.* **1984**, *30*, 578.

(8) Liptak, J.; Nedbal, J.; Ilavsky, M. *Polym. Bull.* **1987**, *18*, 81.

(9) Tanaka, T. *Polymer* **1979**, *20*, 1404.

(10) Lee, K.; Marchetti, M.; Cussler, E. L.; McHugh, M. A. Pressure dependent phase transitions in hydrogels. *Chem. Eng. Sci.*, in press.

(11) Heskins, M.; Guillet, J. E. *J. Macromol. Sci., Chem.* **1968**, *A2*, 1441.

(12) Malcolm, G. N.; Rowlinson, J. S. *Trans. Faraday Soc.* **1957**, *53*, 921.

(13) Freeman, P. I.; Rowlinson, J. S. *Polymer* **1960**, *1*, 20.

(14) Flory, P. J. *Principles of Polymer Chemistry*; Cornell University Press: Ithaca, NY, 1953.

(15) Sanchez, I. C. *Polymer Phase Separation. Preprint for Encyclopedia of Physical Science and Technology*; Academic: New York, 1986.

(16) Erman, B.; Flory, P. J. *Macromolecules* **1986**, *19*, 2342.

(17) James, H.; Guth, E. *J. Chem. Phys.* **1953**, *21*, 1039.

(18) Fox, T. J.; Flory, P. J. *J. Am. Chem. Soc.* **1948**, *70*, 2384.

(19) Flory, P. J. *Proc. R. Soc. London* **1976**, *351*, 351.

(20) Lacombe, R. H.; Sanchez, I. C. *J. Phys. Chem.* **1976**, *80*, 2568.

(21) Sanchez, I. C.; Lacombe, R. H. *Macromolecules* **1976**, *11*, 1145.

(22) Kleintjens, L. A.; Koningsveld, R. Liquid-liquid phase separation in multicomponent polymer systems. XIX. *Mean-field Lattice-gas Treatment of the System n-alkane/linear-polyethylene*; Central Laboratory DSM: The Netherlands, 1979.

(23) Delmas, G.; Patterson, D.; Somcynsky, T. *J. Polym. Sci.* **1962**, *57*, 79.

(24) Flory, P. J.; Orwoll, R. A.; Vrij, A. *J. Am. Chem. Soc.* **1964**, *86*, 3515.

(25) Patterson, D. *Macromolecules* **1969**, *2*, 672.

(26) Flory, P. J. *Rubber Chem. Technol.* **1975**, *48*, 513.

(27) Guth, E. *J. Polym. Sci., Part C* **1966**, *12*, 89.

(28) Trank, S. Ph.D Thesis, University of Minnesota, 1988.

(29) Marchetti, M. Ph.D. Thesis, University of Minnesota, 1989.

(30) Hirotsu, S.; Hirokawa, Y.; Tanaka, T. *J. Chem. Phys.* **1987**, *87*, 1392.

(31) Prange, M.; Hooper, H. H.; Prausnitz, J. M. *AIChE J.* **1989**, *35*, 803.

(32) Hooper, H. H.; Baker, J. P.; Blanch, H. W.; Prausnitz, J. M. Swelling equilibria for positively ionized hydrogels. *Macromolecules*, submitted for publication.

Registry No. Poly(isopropylacrylamide), 25189-55-3.